Electronic Research Archive

https://www.aimspress.com/journal/era

ERA, 34(8): 5267–5285.
DOI: 10.3934/era.2026234
Received: 14 April 2026
Revised: 03 May 2026
Accepted: 18 May 2026
Published: 22 June 2026

Research article

Memory-based switched event-triggered stabilization with switched gains for memristive neural networks

Tianran Bu*

School of Information and Artificial Intelligence, Anhui Business College, Wuhu 241002, China

* **Correspondence:** Email: butianranabc@126.com.

Abstract: This paper investigates the problem of event-triggered stabilization for memristive neural networks (MNNs). To reduce the consumption of limited network communication resources, a memory-based switched event-triggered rule is proposed, in which an integral-type time-memory function is incorporated into the triggering threshold to characterize the average historical state information. The proposed event-triggered rule divides the entire time interval into a variable-length waiting interval and a continuous, event-triggered interval. To enlarge the maximum allowable variable-length waiting interval, a switched controller with different feedback gains is designed for these two intervals. A sufficient condition ensuring asymptotic stability of the closed-loop MNN is derived by constructing a piecewise Lyapunov functional, employing several integral inequalities, and introducing appropriate slack matrices. Subsequently, by decoupling the nonlinearities, a convex matrix-inequalities-based condition is established, enabling the explicit computation of the feedback gains. Finally, a simulation example is provided to demonstrate the effectiveness of the proposed memory-based switched event-triggered stabilization scheme.

Keywords: memristive neural network; switched gain; asymptotic stability; event-triggered control

1. Introduction

The memristor, theoretically introduced by Chua in 1971 as the fourth fundamental circuit element to complement the resistor, capacitor, and inductor [1], remained an abstract concept until HP Labs fabricated the first nanoscale physical device exhibiting memristive characteristics in 2008 [2]. Since then, memristors have garnered significant cross-disciplinary interest due to their unique properties, such as nanoscale dimensions, nonvolatility, and low power consumption. Given their striking functional resemblance to biological synapses, memristors are ideal candidates for simulating neuronal connections. By replacing traditional resistive elements with memristors in recurrent neural networks, memristive neural networks (MNNs) have emerged as a powerful framework. In MNNs, memristive connection weights switch abruptly between distinct values in response to the evolution of system states; consequently, MNNs are inherently state-dependent switched systems. Leveraging these rich dynamical behaviors, MNNs have demonstrated enormous potential across diverse applications.

The stability of MNNs is known as a fundamental prerequisite for their practical applications. Over the past decades, a variety of control strategies have been proposed to stabilize MNNs. For instance, Arslan et al. [3] investigated the fixed-time stabilization of complex-valued MNNs and proposed a state-feedback controller design scheme by decomposing activation functions into real and imaginary components. Sheng et al. [4] examined the exponential stabilization for fuzzy MNNs with multi-delays via an intermittent control strategy. By establishing a novel Razumikhin theorem, Zhang et al. [5] derived several conditions for Mittag-Leffler stabilizing time-delay fractional-order MNNs. Using Green's formula and boundary conditions, Liu et al. [6] focused on Markov jumping MNNs subject to reaction-diffusion terms and proposed a preassigned-time control approach aiming at achieving stability for the resulting synchronization error dynamics. Suvetha et al. [7] presented a fault-tolerant framework to stabilize MNNs with actuator faults and applied it to genetic regulatory models. Driven by the swift evolution of computer technologies and communication engineering, networked control frameworks have received increasing attention for stabilizing MNNs [8–10]. Compared with traditional point-to-point schemes, networked control offers superior efficiency, enhanced reliability, and reduced maintenance overhead [11, 12].

In engineering practice, network bandwidth is typically limited [13]. Early networked control architectures primarily relied on periodic sampled-data schemes. To ensure performance under varying conditions, the sampling interval was often chosen to be conservatively small, leading to redundant packets and network congestion. To address these inefficiencies, Tabuada [14] proposed an event-triggered rule (ETR), wherein data transmission is dictated by state-dependent conditions rather than a fixed temporal schedule. By restricting transmissions to instances where a predefined triggering threshold is breached, ETRs substantially alleviate the communication burden while maintaining prescribed performance levels. Building upon this paradigm, a number of advanced ETRs have recently emerged, including the self-triggered rule [15], periodic ETR [16], disturbance-dependent ETR [17], two-channel ETR [18], dynamic ETR [19], and switched ETRs (SETRs) [20–22]. By combining periodic sampling with continuous event triggering, SETRs guarantee a strictly positive minimum inter-event interval, thus excluding the Zeno phenomenon [23]. Despite this advantage, a common trait of current SETRs is their memoryless nature, which fails to account for the system's historical behavior and can lead to unnecessary triggering during transient fluctuations. Moreover, the majority of SETR frameworks rely on the assumption of a constant waiting interval, which may be infeasible in practice due to intrinsic hardware constraints.

Motivated by these observations, the current work focuses on the stabilization of MNNs within a switched event-triggered framework. The main contributions are summarized below:

1) A memory-based SETR (MBSETR) is proposed, which incorporates an integral-type time-memory function into the triggering threshold to capture historical state information and introduces a variable-length waiting interval. Compared with SETRs in [20–23], the proposed rule can effectively reduce redundant transmissions.

2) A switched controller with two distinct feedback gains is designed to asymptotically stabilize the MNNs. Specifically, one gain is applied during the variable-length waiting interval, while the

other operates in the continuous event-triggered interval. In contrast to the fixed-gain case, the introduction of switched gains contributes to enlarging the maximum allowable bound on the variable-length waiting interval.

2. MNN model and control framework

Throughout, standard notations are used, consistent with those in [24, 25], unless otherwise specified. In particular, the notation $\mathscr{S}(X)$ is used as a shorthand for $X + X^T$ and $*$ in a block matrix denotes the corresponding symmetric term.

The MNN under consideration consists of n neurons, and its dynamics are formulated as

$$\dot{r}_i(t) = -a_i r_i(t) + \sum_{j=1}^{n} b_{ij}(r_i(t)) f_j(r_j(t)) + \sum_{j=1}^{n} c_{ij}(r_i(t)) f_j(r_j(t-\tau(t))) + u_i(t), \tag{2.1}$$

where $r_i(t)$ $(i = 1, \cdots, n)$ characterizes the dynamical state associated with the ith neuron; the positive scalar a_i denotes the self-inhibition coefficient of the ith neuron; $\tau(t)$ serves as the time delay, constrained by $0 \le \tau(t) \le \tau_m$ and $\dot{\tau}(t) \le \lambda < 1$ [26, 27]; $f_j(\cdot)$ stands for the activation function of the jth neuron satisfying $f_j(0) = 0$ [28–30]; the memristive behavior is characterized by state-dependent connection weights $b_{ij}(r_i(t))$ and $c_{ij}(r_i(t))$, given by

$$b_{ij}(r_i(t)) = \begin{cases} b'_{ij}, & |r_i(t)| \le S_i, \\ b''_{ij}, & |r_i(t)| > S_i, \end{cases} \quad c_{ij}(r_i(t)) = \begin{cases} c'_{ij}, & |r_i(t)| \le S_i, \\ c''_{ij}, & |r_i(t)| > S_i, \end{cases}$$

where $S_i > 0$ is switching jump and b'_{ij}, b''_{ij}, c'_{ij}, c''_{ij} are constants satisfying $b'_{ij} \ne b''_{ij}$, $c'_{ij} \ne c''_{ij}$, and $u_i(t)$ is the control input.

Regarding the activation functions, the assumption below is imposed as in [31, 32], which is more general than the conventional Lipschitz condition frequently adopted in the literature [33–35].

Assumption 2.1. *For any distinct $x_1, x_2 \in \mathbb{R}$,*

$$\pi_i^- \le \frac{f_i(x_1) - f_i(x_2)}{x_1 - x_2} \le \pi_i^+$$

holds for $i \in \{1, \cdots, n\}$. Here, π_i^- and π_i^+ are given constants.

Due to the discontinuous nature of the switching weights $b_{ij}(r_i(t))$ and $c_{ij}(r_i(t))$, the MNN model is characterized as a differential equation subject to a non-continuous right-hand side. Consequently, the analysis of MNN (2.1) is conducted through the lens of Filippov's generalized solutions.

Denote $b_{ij} = \max\left\{b'_{ij}, b''_{ij}\right\}$, $\tilde{b}_{ij} = \min\left\{b'_{ij}, b''_{ij}\right\}$, $c_{ij} = \max\left\{c'_{ij}, c''_{ij}\right\}$, $\tilde{c}_{ij} = \min\left\{c'_{ij}, c''_{ij}\right\}$, $\hat{b}_{ij} = \frac{b_{ij}+\tilde{b}_{ij}}{2}$, $\check{b}_{ij} = \frac{b_{ij}-\tilde{b}_{ij}}{2}$, $\hat{c}_{ij} = \frac{c_{ij}+\tilde{c}_{ij}}{2}$, $\check{c}_{ij} = \frac{c_{ij}-\tilde{c}_{ij}}{2}$. Then, in light of differential inclusion and measurable selection theories, and following the procedure described in [36], there are measurable functions $\wedge^1_{ij}(t)$ and $\wedge^2_{ij}(t)$, such that

$$\dot{r}_i(t) = -a_i r_i(t) + \sum_{j=1}^{n} (\hat{b}_{ij} + \check{b}_{ij} \wedge^1_{ij}(t)) f_j(r_j(t)) + \sum_{j=1}^{n} (\hat{c}_{ij} + \check{c}_{ij} \wedge^2_{ij}(t)) f_j(r_j(t-\tau(t))) + u_i(t). \tag{2.2}$$

For compact representation, let

$$\begin{aligned}
r(t) &= [r_1(t), \cdots, r_n(t)]^T, \ A = \mathrm{diag}\{a_1, \cdots, a_n\},\\
u(t) &= [u_1(t), \cdots, u_n(t)]^T, \ f(r(t)) = [f_1(r_1(t)), \cdots, f_n(r_n(t))]^T,\\
B &= [\hat{b}_{ij}]_{n\times n}, \quad C = [\hat{c}_{ij}]_{n\times n},\\
\Lambda_k(t) &= \mathrm{diag}\{\Lambda_{11}^k(t), \cdots, \Lambda_{1n}^k(t), \cdots, \Lambda_{n1}^k(t), \cdots, \Lambda_{nn}^k(t)\},\\
B_1 &= \left[\sqrt{\check{b}_{11}}\varepsilon_1, \cdots, \sqrt{\check{b}_{1n}}\varepsilon_1, \cdots, \sqrt{\check{b}_{n1}}\varepsilon_n, \cdots, \sqrt{\check{b}_{nn}}\varepsilon_n\right]_{n\times n^2},\\
B_2 &= \left[\sqrt{\check{b}_{11}}\varepsilon_1, \cdots, \sqrt{\check{b}_{1n}}\varepsilon_n, \cdots, \sqrt{\check{b}_{n1}}\varepsilon_1, \cdots, \sqrt{\check{b}_{nn}}\varepsilon_n\right]^T_{n\times n^2},\\
C_1 &= \left[\sqrt{\check{c}_{11}}\varepsilon_1, \cdots, \sqrt{\check{c}_{1n}}\varepsilon_1, \cdots, \sqrt{\check{c}_{n1}}\varepsilon_n, \cdots, \sqrt{\check{c}_{nn}}\varepsilon_n\right]_{n\times n^2},\\
C_2 &= \left[\sqrt{\check{c}_{11}}\varepsilon_1, \cdots, \sqrt{\check{c}_{1n}}\varepsilon_n, \cdots, \sqrt{\check{c}_{n1}}\varepsilon_1, \cdots, \sqrt{\check{c}_{nn}}\varepsilon_n\right]^T_{n\times n^2},
\end{aligned}$$

in which $\varepsilon_i \in \mathbb{R}^n$ stand for the standard basis vector with 1 at the i-th position and 0 otherwise and the time-varying matrices $\wedge_k(t)$ are subject to the norm constraint $\wedge_k(t)\wedge_k(t) \leq I$ $(k = 1, 2)$. Consequently, the dynamics in MNN (2.2) can be recast as

$$\dot{r}(t) = -Ar(t) + (B + B_1\wedge_1(t)B_2)f(r(t)) + (C + C_1\wedge_2(t)C_2)f(r(t-\tau(t))) + u(t). \tag{2.3}$$

The objective of this study is to stabilize the MNN (2.1) within an MBSETR, which is detailed as follows: let $\{t_k\}_0^\infty$ denote the triggering instant sequence. Upon a triggering event at t_k, the sampled data $r(t_k)$ is transmitted to the controller, followed by a mandatory waiting interval of length h_k. Once $t \geq t_k + h_k$, the system enters a continuous monitoring phase until the triggering condition is violated at t_{k+1}. The condition to determine the triggering instants is defined by

$$t_{k+1} = \min\{t \geq t_k + h_k \mid (r(t) - r(t_k))^T\Omega(r(t) - r(t_k)) > \alpha\Phi^T(t)\Omega\Phi(t) + \beta e^{-\gamma t}\}, \tag{2.4}$$

where Ω is a positive semi-definite weighting matrix, $\Phi(t) = \frac{1}{m_s}\int_{t-m_s}^t r(s)ds$ with m_s the memory interval, and $\alpha \geq 0, \beta \geq 0, \gamma > 0$ are pre-assigned scalars. The variable-length waiting interval h_k resides in $[h_1, h_2]$, in which h_1 and h_2 $(h_2 \geq h_1 > 0)$ are given scalars, specifying the lower and upper bounds of h_k, respectively. Consequently, for any k, the inter-event time satisfies $t_{k+1} - t_k \geq h_k \geq h_1 > 0$. Since the triggering interval is lower-bounded by a positive constant h_1, the Zeno phenomenon is inherently precluded. The corresponding switched control law is formulated as

$$u(t) = \begin{cases} -K_1 r(t_k), \ t \in [t_k, t_k + h_k), \\ -K_2 r(t_k), \ t \in [t_k + h_k, t_{k+1}) \end{cases} \tag{2.5}$$

with K_1 and K_2 being two different feedback gains to be determined later. A zero-order holder ensures the control signal remains constant between updates.

Remark 2.1. *Compared with some recent ETRs (e.g., those proposed in [37, 38]), it can be observed from the construction of (2.4) that MBSETR incorporates the concepts of switching and time-memory within a unified framework. By alternating between variable-interval sampling and continuous* *event-triggered control, the proposed ETR effectively lightens the network communication burden while inherently precluding the Zeno phenomenon. A key feature is the inclusion of an integral-type time-memory function* $\Phi(t)$*, which captures the average historical state information over the interval* $[t - m_s, t]$*. Furthermore, the threshold function is also enhanced by an exponential term* $\beta e^{-\gamma t}$*. Such a configuration ensures that triggering occurs only when strictly necessary, thereby significantly reducing redundant data transmission. In particular, MBSETR (2.4) simplifies to the decay-included SETR (DISETR) in [20, 21] when* $m_s \to 0$ *and further reduces to the SETR in [22, 23] when* $m_s \to 0$*,* $\beta = 0$*, and* $h_k = h$*.*

Incorporating controller (2.5) into MNN (2.3) results in the switched closed-loop dynamics:

$$\begin{aligned}\dot{r}(t) &= -Ar(t) + (B + B_1 \wedge_1 (t)B_2)f(r(t)) + (C + C_1 \wedge_2 (t)C_2)f(r(t - \tau(t))) \\ &\quad - K_1 r(t - \omega(t)),\ t \in [t_k, t_k + h_k), \qquad (2.6)\\ \dot{r}(t) &= -Ar(t) + (B + B_1 \wedge_1 (t)B_2)f(r(t)) + (C + C_1 \wedge_2 (t)C_2)f(r(t - \tau(t))) \\ &\quad - K_2 r(t_k),\ t \in [t_k + h_k, t_{k+1}). \qquad (2.7)\end{aligned}$$

Here, $\omega(t) \triangleq t - t_k$ serves as the time-varying input delay for $t \in [t_k, t_k + h_k)$, which obviously remains smaller than h_k.

At this stage, the primary objective of this study can be explicitly defined: we intend to stabilize MNN (2.1) by using the MBSETR (2.4) and the switched controller $u(t)$ (2.5). In essence, we seek to ensure that the closed-loop MNN (2.3) achieves global asymptotic stability (GAS) under the established triggering and control constraints.

3. Stability conditions and feedback-gain solving

In what follows, one establishes two sufficient conditions for achieving GAS of closed-loop MNN (2.3). Following this, an expression for determining the switched feedback gains is presented, leaning on the second condition. The derivation process relies on the two fundamental lemmas provided below:

Lemma 3.1. *[39] Considering a matrix* $X > 0$ *and a continuous function* $g(s) : [p, q] \to \mathbb{R}^n$*, one has*

$$-\int_p^q g^T(s)Xg(s)ds \le -\bigg(\int_p^q g(s)ds\bigg)^T X\bigg(\int_p^q g(s)ds\bigg).$$

Lemma 3.2. *[40] Given a matrix* $X > 0$ *and a continuously differentiable function* $g(s) : [p, q] \to \mathbb{R}^n$*,*

$$-\int_p^q \dot{g}^T(s)X\dot{g}(s)ds \le -\frac{1}{q-p}v_0^T \Upsilon(X)v_0$$

holds, in which

$$v_0 = col\bigg\{g(q), g(p), \frac{1}{q-p}\int_p^q g(s)ds\bigg\},\ \Upsilon(X) = \begin{bmatrix} 4X & 2X & -6X \\ * & 4X & -6X \\ * & * & 12X \end{bmatrix}.$$

Theorem 3.1. *Given scalars $\alpha \geq 0$, $\beta \geq 0$, $\gamma > 0$, $\sigma > 0$, $m_s > 0$, and $h_2 \geq h_1 > 0$ and given matrices K_1, K_2, and Ω, closed-loop MNN (2.3) is globally asymptotically stable, if there exists a collection of matrices $P_i > 0$ $(i = 1, \cdots, 6)$, diagonal matrices $M_1 > 0$, $M_2 > 0$, $Y_i > 0$ $(i = 1, \cdots, 4)$, and arbitrary matrices Q_1, Q_2, R_1, R_2, $\forall\ h_k \in \{h_1, h_2\}$, satisfying the following constraints:*

$$S_1(h_k) = \begin{bmatrix} P_1 + h_k \frac{\mathscr{S}(Q_1)}{2} & h_k(-Q_1 + Q_2) \\ * & h_k(-\mathscr{S}(Q_2) + \frac{\mathscr{S}(Q_1)}{2}) \end{bmatrix} > 0, \tag{3.1}$$

$$S_2(h_k) = \begin{bmatrix} \hat{\Sigma}(h_k) & \eta_1 & \eta_2 & \eta_3 & \eta_4 \\ * & -Y_1 & 0 & 0 & 0 \\ * & * & -Y_2 & 0 & 0 \\ * & * & * & -Y_3 & 0 \\ * & * & * & * & -Y_4 \end{bmatrix} < 0, \tag{3.2}$$

$$S_3(h_k) = \begin{bmatrix} \check{\Sigma}(h_k) & \eta_1 & \eta_2 & \eta_3 & \eta_4 \\ * & -Y_1 & 0 & 0 & 0 \\ * & * & -Y_2 & 0 & 0 \\ * & * & * & -Y_3 & 0 \\ * & * & * & * & -Y_4 \end{bmatrix} < 0, \tag{3.3}$$

$$S_4 = \begin{bmatrix} \Theta & \eta_5 & \eta_6 & \eta_7 & \eta_8 \\ * & -Y_1 & 0 & 0 & 0 \\ * & * & -Y_2 & 0 & 0 \\ * & * & * & -Y_3 & 0 \\ * & * & * & * & -Y_4 \end{bmatrix} < 0, \tag{3.4}$$

where $\hat{\Sigma}(h_k) = [\hat{\Sigma}_{ij}]_{10n\times 10n}$, $\check{\Sigma}(h_k) = [\check{\Sigma}_{ij}]_{10n\times 10n}$, *and* $\Theta = [\Theta_{ij}]_{9n\times 9n}$ *are all symmetric matrices with* $\hat{\Sigma}_{11} = 2\sigma P_1 + P_2 + m_s P_4 - \frac{4P_3}{\tau_m} e^{-2\sigma\tau_m} + h_k P_5 + \frac{\sigma h_2 h_k}{2} P_5 - \frac{4P_6}{h_2} e^{-2\sigma h_2} + \frac{2\sigma h_k - 1}{2} \mathscr{S}(Q_1) - \mathscr{S}(R_1^T A) - \Pi_1 M_1$, $\hat{\Sigma}_{12} = P_1 + \frac{h_k}{2} \mathscr{S}(Q_1) + \frac{h_2 h_k}{4} P_5 - R_1^T - AR_2$, $\hat{\Sigma}_{14} = -\frac{2P_6}{h_2} e^{-2\sigma h_2} - R_1^T K_1 + (2\sigma h_k - 1)(-Q_1 + Q_2)$, $\hat{\Sigma}_{15} = \check{\Sigma}_{15} = \Theta_{15} = -\frac{2P_3}{\tau_m} e^{-2\sigma\tau_m}$, $\hat{\Sigma}_{17} = \check{\Sigma}_{17} = \Theta_{17} = \frac{6P_3}{\tau_m} e^{-2\sigma\tau_m}$, $\hat{\Sigma}_{18} = \check{\Sigma}_{18} = \frac{6P_6}{h_2} e^{-2\sigma h_2}$, $\hat{\Sigma}_{19} = \check{\Sigma}_{19} = \Theta_{18} = R_1^T B + \Pi_2 M_1$, $\hat{\Sigma}_{110} = \check{\Sigma}_{110} = \Theta_{19} = R_1^T C$, $\hat{\Sigma}_{22} = \tau_m P_3 + h_k P_6 - \mathscr{S}(R_2)$, $\hat{\Sigma}_{24} = h_k(-Q_1 + Q_2) - R_2^T K_1$, $\hat{\Sigma}_{29} = \check{\Sigma}_{29} = \Theta_{28} = R_2^T B$, $\hat{\Sigma}_{210} = \check{\Sigma}_{210} = \Theta_{29} = R_2^T C$, $\hat{\Sigma}_{33} = \check{\Sigma}_{33} = \Theta_{33} = -(1 - \lambda) e^{-2\sigma\tau_m} P_2 - \Pi_1 M_2$, $\hat{\Sigma}_{310} = \check{\Sigma}_{310} = \Theta_{39} = \Pi_2 M_2$, $\hat{\Sigma}_{44} = -\frac{4P_6}{h_2} e^{-2\sigma h_2} + (2\sigma h_k - 1)(\frac{\mathscr{S}(Q_1)}{2} - \mathscr{S}(Q_2))$, $\hat{\Sigma}_{48} = \check{\Sigma}_{48} = \frac{6P_6}{h_2} e^{-2\sigma h_2}$, $\hat{\Sigma}_{55} = \check{\Sigma}_{55} = \Theta_{55} = -\frac{4P_3}{\tau_m} e^{-2\sigma\tau_m}$, $\hat{\Sigma}_{57} = \check{\Sigma}_{57} = \Theta_{57} = \frac{6P_3}{\tau_m} e^{-2\sigma\tau_m}$, $\hat{\Sigma}_{66} = \check{\Sigma}_{66} = -m_s P_4 e^{-2\sigma m_s}$, $\hat{\Sigma}_{77} = \check{\Sigma}_{77} = -\frac{12P_3}{\tau_m} e^{-2\sigma\tau_m}$, $\hat{\Sigma}_{88} = \check{\Sigma}_{88} = \Theta_{77} = -\frac{12P_6}{h_2} e^{-2\sigma h_2}$, $\hat{\Sigma}_{99} = \check{\Sigma}_{99} = \Theta_{88} = B_2^T (Y_1 + Y_3) B_2 - M_1$, $\hat{\Sigma}_{1010} = \check{\Sigma}_{1010} = \Theta_{99} = C_2^T (Y_2 + Y_4) C_2 - M_2$, $\check{\Sigma}_{11} = \hat{\Sigma}_{11} - 2h_k P_5 - \sigma h_k \mathscr{S}(Q_1)$, $\check{\Sigma}_{12} = \hat{\Sigma}_{12} - \frac{h_k}{2} \mathscr{S}(Q_1)$, $\check{\Sigma}_{14} = \hat{\Sigma}_{14} - 2\sigma h_k(-Q_1 + Q_2)$, $\check{\Sigma}_{22} = \Theta_{22} = \hat{\Sigma}_{22} - h_k P_6$, $\check{\Sigma}_{24} = -R_2^T K_1$, $\check{\Sigma}_{44} = \hat{\Sigma}_{44} + 2\sigma h_k(\mathscr{S}(Q_2) - \frac{\mathscr{S}(Q_1)}{2})$, $\Theta_{11} = 2\sigma P_1 + P_2 + m_s P_4 - \frac{4P_3}{\tau_m} e^{-2\sigma\tau_m} - \Omega - \mathscr{S}(R_1^T A) - \Pi_1 M_1$, $\Theta_{12} = P_1 - R_1^T - AR_2$, $\Theta_{14} = \Omega - R_1^T K_2$, $\Theta_{24} = -R_2^T K_2$, $\Theta_{44} = -\Omega$, $\Theta_{66} = \hat{\Sigma}_{66} + \alpha\Omega$, *other blocks are zero matrices and*

$$\eta_1 = col\left\{R_1^T B_1, 0_{9n\times 2n}\right\},\ \eta_2 = col\left\{R_1^T C_1, 0_{9n\times 2n}\right\},$$
$$\eta_3 = col\left\{0_{n\times 2n}, R_2^T B_1, 0_{8n\times 2n}\right\},\ \eta_4 = col\left\{0_{n\times 2n}, R_2^T C_1, 0_{8n\times 2n}\right\}.$$
$$\eta_5 = col\left\{R_1^T B_1, 0_{8n\times 2n}\right\},\ \eta_6 = col\left\{R_1^T C_1, 0_{8n\times 2n}\right\},$$
$$\eta_7 = col\left\{0_{n\times 2n}, R_2^T B_1, 0_{7n\times 2n}\right\},\ \eta_8 = col\left\{0_{n\times 2n}, R_2^T C_1, 0_{7n\times 2n}\right\},$$

$$\Pi_1 = diag\{\pi_1^-\pi_1^+, \cdots, \pi_n^-\pi_n^+\},\ \Pi_2 = diag\left\{\frac{(\pi_1^- + \pi_1^+)}{2}, \cdots, \frac{(\pi_n^- + \pi_n^+)}{2}\right\}.$$

Proof. Let us consider a candidate piecewise Lyapunov functional defined by

$$\mathcal{V}(t) = \begin{cases} \bar{\mathcal{V}}(t) = \sum_{i=1}^{7} \mathcal{V}_i(t),\ t \in [t_k, t_k + h_k), \\ \widetilde{\mathcal{V}}(t) = \sum_{i=1}^{4} \mathcal{V}_i(t),\ t \in [t_k + h_k, t_{k+1}), \end{cases}$$

where

$$\begin{aligned}
\mathcal{V}_1(t) &= r^T(t)P_1 r(t), \\
\mathcal{V}_2(t) &= \int_{t-\tau(t)}^{t} e^{2\sigma(s-t)} r^T(s)P_2 r(s)ds, \\
\mathcal{V}_3(t) &= \int_{t-\tau_m}^{t}\int_{\theta}^{t} e^{2\sigma(s-t)} \dot{r}^T(s)P_3\dot{r}(s)dsd\theta, \\
\mathcal{V}_4(t) &= \int_{t-m_s}^{t} e^{2\sigma(s-t)}(s - t + m_s) r^T(s)P_4 r(s)ds, \\
\mathcal{V}_5(t) &= \rho(t)\omega(t) r^T(t)P_5 r(t), \\
\mathcal{V}_6(t) &= \rho(t)\int_{t-\omega(t)}^{t} e^{2\sigma(s-t)}\dot{r}^T(s)P_6\dot{r}(s)ds, \\
\mathcal{V}_7(t) &= \rho(t)\begin{bmatrix} r(t) \\ r(t-\omega(t)) \end{bmatrix}^T H \begin{bmatrix} r(t) \\ r(t-\omega(t)) \end{bmatrix},
\end{aligned}$$

with

$$\rho(t) = t_k + h_k - t,\ H = \begin{bmatrix} \frac{\mathscr{S}(Q_1)}{2} & -Q_1 + Q_2 \\ * & -\mathscr{S}(Q_2) + \frac{\mathscr{S}(Q_1)}{2} \end{bmatrix}.$$

The continuity of $\mathcal{V}(t)$ is ensured by the fact that $\mathcal{V}_6(t)$ and $\mathcal{V}_7(t)$ vanish before t_k, $t_k + h_k$ and after t_k, $t_k + h_k$. The functionals $\mathcal{V}_i(t)$ for $i \in \{1, ..., 6\}$ are manifestly positive definite. Furthermore, the positive-definite property of the combined term $\mathcal{V}_1(t) + \mathcal{V}_7(t)$ within $[t_k, t_k + h_k)$ follows directly from inequality (3.1). As a result, $\mathcal{V}(t)$ is positive definite across the entire interval $[t_k, t_{k+1})$.

Given $\dot{\tau}(t) \le \lambda < 1$ and $\omega(t) = t - t_k$, calculating the derivative of $\mathcal{V}_i(t)$ $(i = 1, \cdots, 7)$ leads to

$$\begin{aligned}
\dot{\mathcal{V}}_1(t) &= 2r^T(t)P_1\dot{r}(t), \\
\dot{\mathcal{V}}_2(t) &= -2\sigma\mathcal{V}_2(t) + r^T(t)P_2 r(t) - (1 - \dot{\tau}(t))e^{-2\sigma\tau(t)} r^T(t-\tau(t))P_2 r(t-\tau(t)) \\
&\le -2\sigma\mathcal{V}_2(t) + r^T(t)P_2 r(t) - (1-\lambda)e^{-2\sigma\tau_m} r^T(t-\tau(t))P_2 r(t-\tau(t)), \\
\dot{\mathcal{V}}_3(t) &= -2\sigma\mathcal{V}_3(t) + \tau_m\dot{r}^T(t)P_3\dot{r}(t) - \int_{t-\tau_m}^{t} e^{2\sigma(s-t)}\dot{r}^T(s)P_3\dot{r}(s)ds \\
&\le -2\sigma\mathcal{V}_3(t) + \tau_m\dot{r}^T(t)P_3\dot{r}(t) - e^{-2\sigma\tau_m}\int_{t-\tau_m}^{t}\dot{r}^T(s)P_3\dot{r}(s)ds,
\end{aligned}$$

$$
\begin{aligned}
\dot{\mathcal{V}}_4(t) &= -2\sigma\mathcal{V}_4(t) + m_s r^T(t)P_4 r(t) - \int_{t-m_s}^{t} e^{2\sigma(s-t)} r^T(s)P_4 r(s)ds \\
&\leq -2\sigma\mathcal{V}_4(t) + m_s r^T(t)P_4 r(t) - e^{-2\sigma m_s}\int_{t-m_s}^{t} r^T(s)P_4 r(s)ds, \\
\dot{\mathcal{V}}_5(t) &= (\rho(t) - \omega(t))r^T(t)P_5 r(t) + 2\rho(t)\omega(t)r^T(t)P_5\dot{r}(t), \\
\dot{\mathcal{V}}_6(t) &= -2\sigma\mathcal{V}_6(t) + \rho(t)\dot{r}^T(t)P_6\dot{r}(t) - \int_{t-\omega(t)}^{t} e^{2\sigma(s-t)}\dot{r}^T(s)P_6\dot{r}(s)ds \\
&\leq -2\sigma\mathcal{V}_6(t) + \rho(t)\dot{r}^T(t)P_6\dot{r}(t) - e^{-2\sigma h_2}\int_{t-\omega(t)}^{t} \dot{r}^T(s)P_6\dot{r}(s)ds, \\
\dot{\mathcal{V}}_7(t) &= -\begin{bmatrix} r(t) \\ r(t-\omega(t)) \end{bmatrix}^T H \begin{bmatrix} r(t) \\ r(t-\omega(t)) \end{bmatrix} + \rho(t)[\dot{r}^T(t)\mathscr{S}(Q_1)r(t) + 2\dot{r}^T(t)(-Q_1 + Q_2)r(t-\omega(t))].
\end{aligned}
$$

According to Lemma 3.1, it is straightforward to establish that

$$
-e^{-2\sigma m_s}\int_{t-m_s}^{t} r^T(s)P_4 r(s)ds \leq -\frac{1}{m_s}e^{-2\sigma m_s}\left(\int_{t-m_s}^{t} r(s)ds\right)^T P_4\left(\int_{t-m_s}^{t} r(s)ds\right). \tag{3.5}
$$

Based on Lemma 3.2, it leads to

$$
-\int_{t-\tau_m}^{t} \dot{r}^T(s)P_3\dot{r}(s)ds \leq -\frac{1}{\tau_m}v_1^T(t)\Upsilon(P_3)v_1(t), \tag{3.6}
$$

$$
-\int_{t-\omega(t)}^{t} \dot{r}^T(s)P_6\dot{r}(s)ds \leq -\frac{1}{h_2}v_2^T(t)\Upsilon(P_6)v_2(t), \tag{3.7}
$$

where

$$
\begin{aligned}
v_1(t) &= col\left\{r(t), r(t-\tau_m), \frac{1}{\tau_m}\int_{t-\tau_m}^{t} r(s)ds\right\}, \\
v_2(t) &= col\left\{r(t), r(t-\omega(t)), \frac{1}{\omega(t)}\int_{t-\omega(t)}^{t} r(s)ds\right\}.
\end{aligned}
$$

Besides, let $F(r) = [r, f(r)]^T$. Then, in light of Assumption 2.1, it can be verified that there exist diagonal matrices $M_1 > 0, M_2 > 0$ such that

$$
F^T(r(t))\begin{bmatrix} -\Pi_1 & \Pi_2 \\ * & -I \end{bmatrix} M_1 F(r(t)) \geq 0, \tag{3.8}
$$

$$
F^T(r(t-\tau(t)))\begin{bmatrix} -\Pi_1 & \Pi_2 \\ * & -I \end{bmatrix} M_2 F(r(t-\tau(t))) \geq 0. \tag{3.9}
$$

The next proof proceeds in two stages.

Stage 1: $t \in [t_k, t_k + h_k)$. For MNN (2.6), we utilize Lyapunov functional $\bar{\mathcal{V}}(t)$. Here, by introducing free-weighting matrix R_1 and R_2 of appropriate dimensions, we can write

$$
0 = 2[r^T(t)R_1^T + \dot{r}^T(t)R_2^T][-\dot{r}(t) - Ar(t) + B(t)f(r(t)) + C(t)f(r(t-\tau(t))) - K_1 r(t-\omega(t))],
$$

where $B(t) = B + B_1\wedge_1(t)B_2$ and $C(t) = C + C_1\wedge_2(t)C_2$. Also, for diagonal matrices $Y_i > 0, i = 1, \cdots, 4$, with appropriate dimensions, it follows

$$\begin{aligned}
&2r^T(t)R_1^T B_1\wedge_1(t)(t)B_2 f(r(t)) \\
\le\, & f^T(r(t))B_2^T Y_1 B_2 f(r(t)) + r^T(t)R_1^T B_1\wedge_1(t)Y_1^{-1}\wedge_1(t)B_1^T R_1 r(t). \\
&2r^T(t)R_1^T C_1\wedge_2(t)(t)C_2 f(r(t-\tau(t))) \\
\le\, & f^T(r(t-\tau(t)))C_2^T Y_2 C_2 f(r(t-\tau(t))) + r^T(t)R_1^T C_1\wedge_2(t)Y_2^{-1}\wedge_2(t)C_1^T R_1 r(t). \\
&2\dot{r}^T(t)R_2^T B_1\wedge_1(t)(t)B_2 f(r(t)) \\
\le\, & f^T(r(t))B_2^T Y_3 B_2 f(r(t)) + \dot{r}^T(t)R_2^T B_1\wedge_1(t)Y_3^{-1}\wedge_1(t)B_1^T R_2\dot{r}(t). \\
&2\dot{r}^T(t)R_2^T C_1\wedge_2(t)(t)C_2 f(r(t-\tau(t))) \\
\le\, & f^T(r(t-\tau(t)))C_2^T Y_4 C_2 f(r(t-\tau(t))) + \dot{r}^T(t)R_2^T C_1\wedge_2(t)Y_4^{-1}\wedge_2(t)C_1^T R_2\dot{r}(t).
\end{aligned}$$

Combining the above inequalities and noting that $\wedge_k(t)\wedge_k(t) \le I(k = 1, 2)$ yields

$$\begin{aligned}
&2[r^T(t)R_1^T + \dot{r}^T(t)R_2^T][-\dot{r}(t) - Ar(t) + B(t)f(r(t)) + C(t)f(r(t-\tau(t))) - K_1 r(t-\omega(t))] \\
\le\, & 2[r^T(t)R_1^T + \dot{r}^T(t)R_2^T][-\dot{r}(t) - Ar(t) + Bf(r(t)) + Cf(r(t-\tau(t))) - K_1 r(t-\omega(t))] \\
&+ r^T(t)R_1^T[B_1Y_1^{-1}B_1^T + C_1Y_2^{-1}C_1^T]R_1 r(t) + \dot{r}^T(t)R_2^T[B_1Y_3^{-1}B_1^T + C_1Y_4^{-1}C_1^T]R_2\dot{r}(t) \\
&+ f^T(r(t))B_2^T[Y_1 + Y_3]B_2 f(r(t)) + f^T(r(t-\tau(t)))C_2^T[Y_2 + Y_4]C_2 f(r(t-\tau(t))).
\end{aligned} \tag{3.10}$$

From inequalities (3.5)–(3.10) we arrive at

$$\dot{\bar{\mathcal{V}}}(t) + 2\sigma\bar{\mathcal{V}}(t) \le \xi_1^T(t)[\frac{\rho_(t)}{h_k}(\hat{\Sigma}(h_k) + \Xi) + \frac{\omega(t)}{h_k}(\check{\Sigma}(h_k) + \Xi)]\xi_1(t),$$

where $\xi_1(t) = col\Big\{r(t), \dot{r}(t), r(t-\tau(t)), r(t-\omega(t)), r(t-\tau_m), \frac{1}{m_s}\int_{t-m_s}^t r(s)ds, \frac{1}{\tau_m}\int_{t-\tau_m}^t r(s)ds, \frac{1}{\omega(t)}\int_{t-\omega(t)}^t r(s)ds, f(r(t)), f(r(t-\tau(t)))\Big\}$, and $\Xi = \eta_1 Y_1^{-1}\eta_1^T + \eta_2 Y_2^{-1}\eta_2^T + \eta_3 Y_3^{-1}\eta_3^T + \eta_4 Y_4^{-1}\eta_4^T$. By invoking Schur's complement, $\hat{\Sigma}(h_k) + \Xi < 0$ and $\check{\Sigma}(h_k) + \Xi < 0$ can be transformed into the equivalent forms presented in (3.2) and (3.3), respectively. Thus, we obtain

$$\dot{\bar{\mathcal{V}}}(t) + 2\sigma\bar{\mathcal{V}}(t) \le 0,\ t \in [t_k, t_k + h_k).$$

Integrating the aforementioned inequality from t_k till t results in

$$\bar{\mathcal{V}}(t) \le \bar{\mathcal{V}}(t_k)e^{-2\sigma(t-t_k)}. \tag{3.11}$$

Stage 2: $t \in [t_k + h_k, t_{k+1})$. Here, the attention shifts to $\widetilde{\mathcal{V}}(t)$ for MNN (2.7). By introducing free-weighting matrices R_1 and R_2 of appropriate dimensions, we get

$$0 = 2[r^T(t)R_1^T + \dot{r}^T(t)R_2^T][-\dot{r}(t) - Ar(t) + B(t)f(r(t)) + C(t)f(r(t-\tau(t))) - K_2 r(t_k)].$$

Combining (2.4) and (3.5)–(3.10) gives rise to

$$\dot{\widetilde{\mathcal{V}}}(t) + 2\sigma\widetilde{\mathcal{V}}(t) \le \xi_2^T(t)(\Theta + \Theta_0)\xi_2(t) + \beta e^{-\gamma t},$$

where $\Theta_0 = \eta_5 Y_1^{-1}\eta_5^T + \eta_6 Y_2^{-1}\eta_6^T + \eta_7 Y_3^{-1}\eta_7^T + \eta_8 Y_4^{-1}\eta_8^T$ and $\xi_2(t) = col\{r(t), \dot{r}(t), r(t-\tau(t)), r(t_k), r(t-\tau_m), \frac{1}{m_s}\int_{t-m_s}^{t} r(s)ds, \frac{1}{\tau_m}\int_{t-\tau_m}^{t} r(s)ds, f(r(t)), f(r(t-\tau(t)))\}$. With the aid of the Schur complement, $\Theta + \Theta_0 < 0$ can be rewritten as (3.4), which leads to

$$\dot{\widetilde{\mathcal{V}}}(t) + 2\sigma\widetilde{\mathcal{V}}(t) \le \beta e^{-\gamma t}, \quad t \in [t_k + h_k, t_{k+1}).$$

Integrating the aforementioned inequality from $t_k + h_k$ till t results in

$$\widetilde{\mathcal{V}}(t) \le \widetilde{\mathcal{V}}(t_k + h_k)e^{-2\sigma(t-t_k-h_k)} + \int_{t_k+h_k}^{t} \beta e^{-2\sigma(t-s)}e^{-\gamma s}ds. \tag{3.12}$$

Given the continuity of $\mathcal{V}(t)$ at both t_k and $t_k + h_k$, its continuous property can be extended to the entire time domain $[0, +\infty)$. For $t \in [t_k + h_k, t_{k+1})$, the following holds:

$$\begin{aligned}
\mathcal{V}(t) &\overset{(3.12)}{\le} \mathcal{V}(t_k + h_k)e^{-2\sigma(t-t_k-h_k)} + \int_{t_k+h_k}^{t} \beta e^{-2\sigma(t-s)}e^{-\gamma s}ds \\
&\overset{(3.11)}{\le} \mathcal{V}(t_k)e^{-2\sigma(t-t_k)} + \int_{t_k+h_k}^{t} \beta e^{-2\sigma(t-s)}e^{-\gamma s}ds \\
&\le \mathcal{V}(t_k)e^{-2\sigma(t-t_k)} + \int_{t_k}^{t} \beta e^{-2\sigma(t-s)}e^{-\gamma s}ds \\
&\le \mathcal{V}(t_{k-1} + h_{k-1})e^{-2\sigma(t-t_{k-1}-h_{k-1})} \\
&\quad + \int_{t_{k-1}+h_{k-1}}^{t} \beta e^{-2\sigma(t-s)}e^{-\gamma s}ds \\
&\le \mathcal{V}(t_{k-1})e^{-2\sigma(t-t_{k-1})} + \int_{t_{k-1}}^{t} \beta e^{-2\sigma(t-s)}e^{-\gamma s}ds \\
&\le \cdots \le \mathcal{V}(0)e^{-2\sigma t} + \int_{0}^{t} \beta e^{-2\sigma(t-s)}e^{-\gamma s}ds.
\end{aligned}$$

If $t \in [t_k, t_k + h_k)$, by applying a similar derivation as above, the same conclusion can be drawn. To sum up, we are able to conclude that

$$\mathcal{V}(t) \le \begin{cases} (\mathcal{V}(0) - \frac{\beta}{2\sigma-\gamma})e^{-2\sigma t} + \frac{\beta}{2\sigma-\gamma}e^{-\gamma t}, & \gamma \ne 2\sigma, \\ (\mathcal{V}(0) + \beta t)e^{-2\sigma t}, & \gamma = 2\sigma. \end{cases}$$

Since $t \to +\infty$, $e^{-2\sigma t} \to 0$, $e^{-\gamma t} \to 0$, and $te^{-2\sigma t} \to 0$, the GAS of MNN (2.3) is established, thereby completing the proof. □

Remark 3.1. *One should observe that closed-loop MNN (2.3) is inherently a time-dependent switched system resulting from the combined effect of MBSETR (2.4) and switched controller (2.5). Constructing an appropriate Lyapunov functional for such a system is non-trivial. Inspired by [20–23], this work introduces a piecewise-defined Lyapunov functional $\mathcal{V}(t)$, which switches between a time-dependent form $\bar{\mathcal{V}}(t)$ over the variable-interval sampling period and a time-independent form $\widetilde{\mathcal{V}}(t)$ over the triggering interval. The inclusion of $\mathcal{V}_4(t), \cdots, \mathcal{V}_7(t)$, incorporating the available state information over $[t - m_s, t]$, as well as the endpoints t_k, $t_k + h_k$, contributes to reducing the conservativeness of the obtained results.*

Remark 3.2. *Note that $S_i(h_k)$ $(i = 1, 2, 3)$ can be represented as a linear combination of $S_i(h_1)$ and $S_i(h_2)$ by the Schur complement and matrix decomposition techniques. To be specific, $S_i(h_k) = \vartheta S_i(h_1) + (1 - \vartheta)S_i(h_2)$ for $0 \leq \vartheta \leq 1$. Meanwhile, S_4 does not depend on h_k. Hence, (3.1)–(3.4) are still feasible for all $h_k \in [h_1, h_2]$.*

Theorem 3.2. *Given a set of prescribed scalars $\alpha \geq 0$, $\beta \geq 0$, $\gamma > 0$, $\sigma > 0$, $m_s > 0$, $h_2 \geq h_1 > 0$, and $\theta > 0$, closed-loop MNN (2.3) is globally asymptotically stable, if there exist a collection of matrices $P_i > 0$ $(i = 1, \cdots, 6)$, $\Omega \geq 0$, diagonal matrices $M_1 > 0$, $M_2 > 0$, $Y_i > 0$ $(i = 1, \cdots, 4)$, and arbitrary matrices Q_1, Q_2, R_1, W_1, W_2, $\forall\ h_k \in \{h_1, h_2\}$, satisfying the following convex matrix-inequalities-based constraints:*

$$S_1(h_k) > 0, S_2(h_k) < 0, S_3(h_k) < 0, S_4 < 0, \tag{3.13}$$

where $\hat{\Sigma}_{12} = P_1 + \frac{h_k}{2}\mathscr{S}(Q_1) + \frac{h_2 h_k}{4}P_5 - R_1^T - \theta AR_1$, $\hat{\Sigma}_{14} = -\frac{2P_6}{h_2}e^{-2\sigma h_2} - W_1 + (2\sigma h_k - 1)(-Q_1 + Q_2)$, $\hat{\Sigma}_{22} = \tau_m P_3 + h_k P_6 - \mathscr{S}(\theta R_1)$, $\hat{\Sigma}_{24} = h_k(-Q_1 + Q_2) - \theta W_1$, $\hat{\Sigma}_{29} = \check{\Sigma}_{29} = \Theta_{28} = \theta R_1^T B$, $\hat{\Sigma}_{210} = \check{\Sigma}_{210} = \Theta_{29} = \theta R_1^T C$, $\check{\Sigma}_{12} = \hat{\Sigma}_{12} - \frac{h_k}{2}\mathscr{S}(Q_1)$, $\check{\Sigma}_{14} = \hat{\Sigma}_{14} - 2\sigma h_k(-Q_1 + Q_2)$, $\check{\Sigma}_{22} = \Theta_{22} = \hat{\Sigma}_{22} - h_k P_6$, $\check{\Sigma}_{24} = -\theta W_1$, $\Theta_{12} = P_1 - R_1^T - \theta AR_1$, $\Theta_{14} = \Omega - W_2$, $\Theta_{24} = -\theta W_2$, and $\eta_3 = col\left\{0_{n\times 2n}, \theta R_1^T B_1, 0_{8n\times 2n}\right\}$, $\eta_4 = col\left\{0_{n\times 2n},\ \theta R_1^T C_1,\ 0_{8n\times 2n}\right\}$, $\eta_7 = col\{0_{n\times 2n},\ \theta R_1^T B_1, 0_{7n\times 2n}\}$, $\eta_8 = col\{0_{n\times 2n}, \theta R_1^T C_1, 0_{7n\times 2n}\}$, and the remaining terms are the same as the corresponding elements in Theorem 3.1. Then, the desired switched feedback gains K_1 and K_2 are designed as

$$K_1 = (R_1^T)^{-1}W_1, \quad K_2 = (R_1^T)^{-1}W_2. \tag{3.14}$$

Proof. Let $R_2 = \theta R_1$, $R_1^T K_1 = W_1$, and $R_1^T K_2 = W_2$. It is easy to see that inequalities in (3.13) can ensure inequalities (3.1)–(3.4) in Theorem 3.1 hold, respectively. □

Remark 3.3. *Theorems 3.1 and 3.2 provide two distinct sufficient conditions for the stability of closed-loop MNN (2.3). Specifically, Theorem 3.1 offers less conservative results; however, the inequalities therein involve coupling terms between the decision variables and control gains K_1 and K_2. Unless these gains are pre-assigned, Theorem 3.1 is difficult to verify directly. In contrast, the matrix inequalities in Theorem 3.2 are convex, allowing the feasibility of the conditions to be readily checked using standard convex optimization solvers, such as YALMIP, MOSEK, and SeDuMi. Moreover, when the inequalities in Theorem 3.2 are satisfied, the desired feedback gains can be explicitly obtained through the mathematical expressions provided in (3.14), which facilitates direct controller synthesis.*

If a non-switched controller of the following form is designed:

$$u(t) = -Kr(t_k),\ t \in [t_k, t_{k+1}), \tag{3.15}$$

where K is the feedback gain to be determined. The design scheme for K is proposed in the upcoming Corollary 3.1 using a similar manner as in Theorem 3.2.

Corollary 3.1. *Given a set of prescribed scalars $\alpha \geq 0$, $\beta \geq 0$, $\gamma > 0$, $\sigma > 0$, $h_2 \geq h_1 > 0$, and $\theta > 0$, closed-loop MNN (2.3) is globally asymptotically stable, if there exist a collection of matrices $P_i > 0$ $(i = 1, 2, \cdots, 6)$, $\Omega \geq 0$, diagonal matrices $M_1 > 0$, $M_2 > 0$, $Y_i > 0$ $(i = 1, 2, \cdots, 4)$, and* *arbitrary matrices Q_1, Q_2, R_1, W, $\forall\ h_k \in \{h_1, h_2\}$, satisfying the following convex matrix-inequalities-based constraints:*

$$S_1(h_k) > 0, S_2(h_k) < 0, S_3(h_k) < 0, S_4 < 0, \tag{3.16}$$

where $\hat{\Sigma}_{14} = -\frac{2P_6}{h_2}e^{-2\sigma h_2} - W + (2\sigma h_k - 1)(-Q_1 + Q_2)$, $\hat{\Sigma}_{24} = h_k(-Q_1 + Q_2) - \theta W$, $\check{\Sigma}_{14} = \hat{\Sigma}_{14} - 2\sigma h_k(-Q_1 + Q_2)$, $\check{\Sigma}_{24} = -\theta W$, $\Theta_{14} = \Omega - W$, $\Theta_{24} = -\theta W$, *and the remaining terms are the same as the corresponding elements in Theorem 3.2. Then, the desired feedback K is designed as*

$$K = (R_1^T)^{-1} W.$$

4. Numerical simulation

This section provides a numerical example to validate the effectiveness of the proposed MBSETR-based stabilization scheme. All numerical calculations and simulations are conducted using MATLAB R2020B, with the YALMIP and MOSEK toolboxes employed to solve the derived conditions.

Take MNN (2.1) with $n = 2, f_j(r_j) = \tanh(r_j), \tau(t) = \frac{e^t}{1+e^t} \leq 1$, and the following parameter values and initial condition into account:

$$b_{11}(r_1(t)) = \begin{cases} -1.8, & |r_1(t)| \leq 1, \\ -1.5, & |r_1(t)| > 1, \end{cases} \quad b_{12}(r_1(t)) = \begin{cases} 2.7, & |r_1(t)| \leq 1, \\ 2.3, & |r_1(t)| > 1, \end{cases}$$
$$b_{21}(r_2(t)) = \begin{cases} 0.8, & |r_2(t)| \leq 1, \\ 0.4, & |r_2(t)| > 1, \end{cases} \quad b_{22}(r_2(t)) = \begin{cases} -0.4, & |r_2(t)| \leq 1, \\ -0.2, & |r_2(t)| > 1, \end{cases}$$
$$c_{11}(r_1(t)) = \begin{cases} -0.3, & |r_1(t)| \leq 1, \\ -0.2, & |r_1(t)| > 1, \end{cases} \quad c_{12}(r_1(t)) = \begin{cases} 0.4, & |r_1(t)| \leq 1, \\ 0.3, & |r_1(t)| > 1, \end{cases}$$
$$c_{21}(r_2(t)) = \begin{cases} 0.1, & |r_2(t)| \leq 1, \\ 0.2, & |r_2(t)| > 1, \end{cases} \quad c_{22}(r_2(t)) = \begin{cases} -2.6, & |r_2(t)| \leq 1, \\ -2.4, & |r_2(t)| > 1, \end{cases}$$
$$a_1 = a_2 = 1.05, \ r(0) = [-0.2, 0.1]^T.$$

Figure 1 depicts the time evolution curves of the state for MNN (2.1) with the aforementioned parameters. It is clear that the MNN fails to maintain stability without the intervention of a control signal. By calculation, it shows that $\tau_m = 1, \lambda = 0.25$, and

$$\Pi_1 = diag\{0, 0\}, \ \Pi_2 = diag\{0.5, 0.5\},$$
$$B = \begin{bmatrix} -1.65 & 2.5 \\ 0.6 & -0.3 \end{bmatrix}, \ C = \begin{bmatrix} -0.25 & 0.35 \\ 0.15 & -2.5 \end{bmatrix},$$
$$B_1 = \begin{bmatrix} \sqrt{0.15} & \sqrt{0.2} & 0 & 0 \\ 0 & 0 & \sqrt{0.2} & \sqrt{0.1} \end{bmatrix},$$
$$C_1 = \begin{bmatrix} \sqrt{0.05} & \sqrt{0.05} & 0 & 0 \\ 0 & 0 & \sqrt{0.05} & \sqrt{0.1} \end{bmatrix},$$
$$B_2 = \begin{bmatrix} \sqrt{0.15} & 0 & \sqrt{0.2} & 0 \\ 0 & \sqrt{0.2} & 0 & \sqrt{0.1} \end{bmatrix}^T,$$

$$C_2 = \begin{bmatrix} \sqrt{0.05} & 0 & \sqrt{0.05} & 0 \\ 0 & \sqrt{0.05} & 0 & \sqrt{0.1} \end{bmatrix}^T.$$

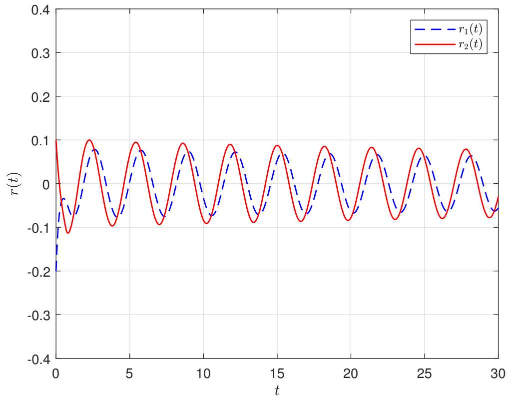

Figure 1. Time evolution curves of state without control input.

In what follows, we demonstrate the effectiveness and superior performance of our control scheme. Let $\alpha = 0.1, \beta = 0.1, \gamma = 1, \theta = 0.2, m_s = 0.5, h_1 = 0.01, h_2 = 0.1$, and $\sigma = 0.2$. Solving the LMIs in (3.13) of Theorem 3.2 gives

$$K_1 = \begin{bmatrix} 2.5956 & 0.81287 \\ 0.2292 & 4.8886 \end{bmatrix}, K_2 = \begin{bmatrix} 1.0450 & 0.1812 \\ 0.0252 & 2.7325 \end{bmatrix},$$
$$\Omega = \begin{bmatrix} 0.4865 & 0.0267 \\ 0.0267 & 0.6564 \end{bmatrix}.$$

While, by solving LMIs (3.16) in Corollary 3.1, the feedback and trigger matrices can be calculated as

$$K = \begin{bmatrix} 2.5983 & 0.8467 \\ 0.2553 & 5.1646 \end{bmatrix}, \Omega = \begin{bmatrix} 0.6377 & 0.1123 \\ 0.1123 & 0.9954 \end{bmatrix}.$$

For simplicity and without loss of generality, h_k is randomly generated within $[h_1, h_2]$ in the simulations. Under the MBSETR (2.4) and switched controller (2.5) with the above trigger matrix and feedback gains, the temporal evolution of the closed-loop MNN states and the associated control input are depicted in Figures 2 and 3. The triggering intervals of MBSETR are given in Figure 4. It is shown that state trajectories asymptotically approach zero under the developed control law, which adequately illustrates the validity of the presented controller design.

To demonstrate the advantages of the proposed MBSETR (2.4), the total number of triggers T_t obtained from Theorem 3.2 is compared with existing SETRs [20–23] under identical simulation settings, including system parameters and initial states. By ensuring the GAS of the closed-loop MNN across all schemes, the comparative results are summarized in Table 1 for different decay rates σ and event threshold parameters α. It can be clearly seen from Table 1 that the proposed MBSETR achieves the lowest trigger times under all values of σ and α, demonstrating its superior performance in reducing unnecessary event triggers. For all three schemes, the triggering frequency decreases as α increases, which is fully consistent with the core mechanism of ETRs.

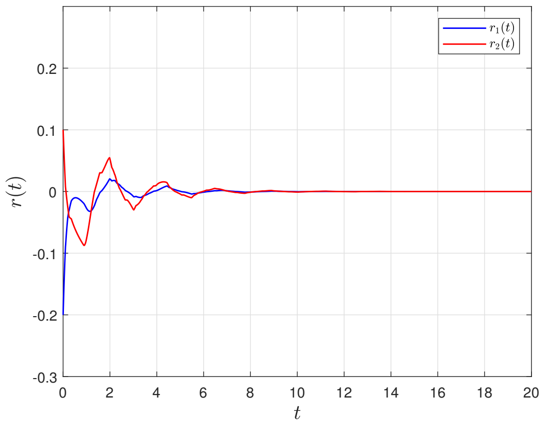

Figure 2. Time evolution curves of closed-loop MNN.

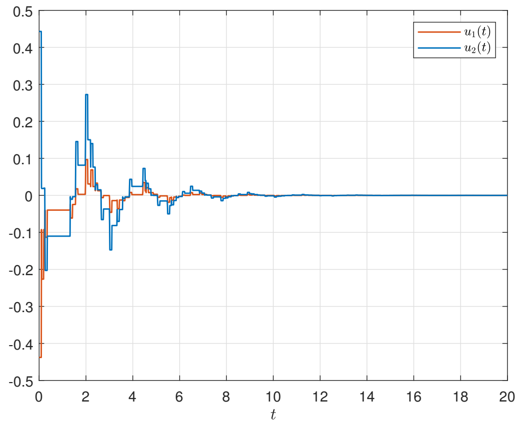

Figure 3. Control input of closed-loop MNN.

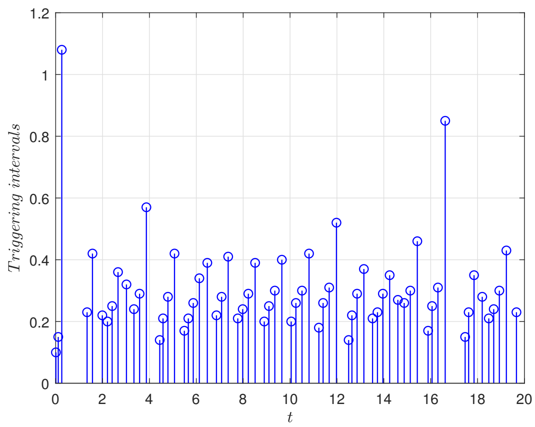

Figure 4. Triggering interval of MBSETR.

To highlight the benefits of switched gains, Table 2 compares the maximum allowable upper bound of h_2 derived from Theorem 3.2 and Corollary 3.1 under different values of α. Clearly, the results obtained from Theorem 3.2 allow a larger upper bound of h_2 than those of Corollary 3.1, confirming that the introduction of switched gains enhances the tolerance for waiting intervals.

Table 1. Comparisons of the number of triggers T_t under different σ and α.

σ	Scheme	T_t for different α				
		$\alpha = 0.1$	$\alpha = 0.15$	$\alpha = 0.2$	$\alpha = 0.25$	$\alpha = 0.3$
	MBSETR (2.4)	96	88	81	76	72
0.10	DISETR [20,21]	104	96	89	84	79
	SETR [22,23]	162	142	122	113	102
	MBSETR (2.4)	92	86	80	75	72
0.12	DISETR [20,21]	100	93	86	83	81
	SETR [22,23]	159	144	130	120	109
	MBSETR (2.4)	85	82	79	75	72
0.14	DISETR [20,21]	94	92	91	85	79
	SETR [22,23]	154	142	131	116	102

Table 2. Comparisons of the maximum allowable upper bound of h_2 with different α.

Methods	$\alpha = 0.1$	$\alpha = 0.2$	$\alpha = 0.3$
Theorem 3.2	0.1563	0.1462	0.1392
Corollary 3.1	0.1328	0.1236	0.1151

5. Conclusions

This paper has addressed the problem of event-triggered stabilization for MNNs. To reduce the consumption of limited network communication resources, an MBSETR has been proposed in (2.4), in which an integral-type time-memory function is incorporated into the triggering threshold to characterize the average historical state information. The proposed event-triggered rule divides the entire time interval into a variable-length waiting interval h_k and a continuous, event-triggered interval $[t_k + h_k, t_{k+1})$. To enlarge the maximum allowable variable-length waiting interval, a switched controller with different feedback gains has been designed in (2.5) for these two intervals. A sufficient condition ensuring the GAS of closed-loop MNN has been derived in Theorem 3.1 by constructing a piecewise Lyapunov functional, employing several integral inequalities, and introducing appropriate slack matrices. Subsequently, by decoupling the nonlinearities, a convex matrix-inequalities-based condition has been proposed in Theorem 3.2, enabling the explicit computation of the feedback gains. Finally, a simulation example has confirmed the superior performance of the proposed memory-based switched event-triggered stabilization scheme. Future research will focus on extending the MBSETR to more complex MNNs to account for uncertainties and external disturbances.

Use of AI tools declaration

The author declares that he has not used Artificial Intelligence (AI) tools in the creation of this article.

Acknowledgments

This work was supported by the Key Project of Natural Science Research in Colleges and Universities of Anhui Province (Grant Nos. 2023AH052297 and 2023AH052299).

Conflict of interest

The author declares there is no conflict of interest.

References

1. L. Chua, Memristor-the missing circuit element, *IEEE Trans. Circuit Theory*, **18** (1971), 507–519. https://doi.org/10.1109/TCT.1971.1083337
2. D. B. Strukov, G. S. Snider, D. R. Stewart, R. S. Williams, The missing memristor found, *Nature*, **453** (2008), 80–83. https://doi.org/10.1038/nature06932
3. E. Arslan, G. Narayanan, M. S. Ali, S. Arik, S. Saroha, Controller design for finite-time and fixed-time stabilization of fractional-order memristive complex-valued bam neural networks with uncertain parameters and time-varying delays, *Neural Networks*, **130** (2020), 60–74. https://doi.org/10.1016/j.neunet.2020.06.021
4. Y. Sheng, T. Huang, Z. Zeng, Exponential stabilization of fuzzy memristive neural networks with multiple time delays via intermittent control, *IEEE Trans. Syst. Man Cybern. Syst.*, **52** (2022), 3092–3101. https://doi.org/10.1109/TSMC.2021.3062381
5. S. Zhang, M. Tang, X. Liu, X. Zhang, Mittag-Lefflerstability and stabilization of delayed fractional-order memristive neural networks based on a new Razumikhin-type theorem, *J. Franklin Inst.*, **361** (2024), 1211–1226. https://doi.org/10.1016/j.jfranklin.2024.01.008
6. H. Liu, J. Cheng, J. Cao, I. Katib, Preassigned-time synchronization for complex-valued memristive neural networks with reaction-diffusion terms and Markov parameters, *Neural Networks*, **169** (2024), 520–531. https://doi.org/10.1016/j.neunet.2023.11.011
7. R. Suvetha, Y. Ma, P. Prakash, Fault tolerant control design for memristive bidirectional associative memory neural networks and its application in genetic regulatory networks, *Neural Comput. Appl.*, **38** (2026), 136. https://doi.org/10.1007/s00521-025-11811-4
8. N. Liu, J. Cheng, Y. Chen, H. Yan, D. Zhang, W. Qi, Adaptive protocol-based control for reaction-diffusion memristive neural networks with semi-Markov switching parameters, *Inf. Sci.*, **677** (2024), 120947. https://doi.org/10.1016/j.ins.2024.120947
9. S. Xiao, Z. Wang, X. Si, G. Liu, Mean-square exponential stabilization of memristive neural networks: Dealing with replay attacks and communication interruptions, *Commun. Nonlinear Sci. Numer. Simul.*, **138** (2024), 108188. https://doi.org/10.1016/j.cnsns.2024.108188

10. Y. Zhang, F. Kong, Q. Zhu, T. Huang, Quantized control based on stabilization of discontinuous memristor-based fuzzy inertial neural networks with proportional delays, *IEEE Trans. Syst. Man Cybern. Syst.*, **54** (2024), 5756–5767. https://doi.org/10.1109/TSMC.2024.3408469
11. X. Zhang, Q. Han, X. Ge, D. Ding, L. Ding, D. Yue, et al., Networked control systems: A survey of trends and techniques, *IEEE/CAA J. Autom. Sin.*, **7** (2020), 1–17. https://doi.org/10.1109/JAS.2019.1911651
12. Y. Wang, S. Wu, C. Lei, J. Jiao, Q. Zhang, A review on wireless networked control system: The communication perspective, *IEEE Internet Things J.*, **11** (2024), 7499–7524. https://doi.org/10.1109/JIOT.2023.3342032
13. K. Liu, E. Fridman, Y. Xia, *Networked Control Under Communication Constraints: A Time-Delay Approach*, 1^{st} edition, Springer, 2020. https://doi.org/10.1007/978-981-15-4230-5
14. P. Tabuada, Event-triggered real-time scheduling of stabilizing control tasks, *IEEE Trans. Autom. Control*, **52** (2007), 1680–1685. https://doi.org/10.1109/TAC.2007.904277
15. L. Zhang, S. Xu, Static pinning synchronization control of self-triggered coupling dynamical networks, *Neural Networks*, **182** (2025), 106798. https://doi.org/10.1016/j.neunet.2024.106798
16. B. Jiang, J. Wei, Y. Liu, W. Gui, Periodic event-triggered impulsive control of linear uncertain systems, *IEEE Trans. Autom. Sci. Eng.*, **22** (2024), 6876–6883. https://doi.org/10.1109/TASE.2024.3456125
17. W. Wu, L. He, Z. Yan, J. Zhou, Event-triggered extended dissipativity stabilization of semi-Markov switching systems, *Appl. Math. Modell.*, **118** (2023), 618–640. https://doi.org/10.1016/j.apm.2023.01.045
18. X. Chen, S. Hu, T. Yang, X. Xie, J. Qiu, Event-triggered bipartite consensus of multiagent systems with input saturation and DoS attacks over weighted directed networks, *IEEE Trans. Syst. Man Cybern. Syst.*, **54** (2024), 4054–4065. https://doi.org/10.1109/TSMC.2024.3377213
19. C. Yi, J. Cai, R. Guo, Synchronization of a class of nonlinear multiple neural networks with delays via a dynamic event-triggered impulsive control strategy, *Electron. Res. Arch.*, **32** (2024), 4581–4603. https://doi.org/10.3934/era.2024208
20. Y. Wang, H. Tuo, H. Lyu, Z. Cheng, Y. Xin, Aperiodic switching event-triggered stabilization of continuous memristive neural networks with interval delays, *Neural Networks*, **164** (2023), 264–274. https://doi.org/10.1016/j.neunet.2023.04.036
21. Z. Yan, X. Huang, J. Cao, Variable-sampling-period dependent global stabilization of delayed memristive neural networks based on refined switching event-triggered control, *Sci. China Inf. Sci.*, **63** (2020), 212201. https://doi.org/10.1007/s11432-019-2664-7
22. Z. Fei, C. Guan, H. Gao, Exponential synchronization of networked chaotic delayed neural network by a hybrid event trigger scheme, *IEEE Trans. Neural Networks Learn. Syst.*, **29** (2018), 2558–2567. https://doi.org/10.1109/TNNLS.2017.2700321
23. A. Selivanov E. Fridman, Event-triggered H_∞ control: A switching approach, *IEEE Trans. Autom. Control*, **61** (2016), 3221–3226. https://doi.org/10.1109/TAC.2015.2508286

24. J. Zhou, J. Dong, S. Xu, C. K. Ahn, Input-to-state stabilization for Markov jump systems with dynamic quantization and multimode injection attacks, *IEEE Trans. Syst. Man Cybern. Syst.*, **54** (2024), 2517–2529. https://doi.org/10.1109/TSMC.2023.3344869

25. Y. Liu, P. Zhang, S. Lee, X. Xie, Observer-based adaptive event-triggered control for interval type-2 fuzzy systems under multiple cyber-attacks, *IEEE Trans. Fuzzy Syst.*, **32** (2024), 2438–2447. https://doi.org/10.1109/TFUZZ.2024.3354241

26. Y. Zhou, X. Chang, J. H. Park, Quantized asynchronous filtering for fuzzy semi-Markov switching systems with multiple stochastic delays under deception attacks, *IEEE Trans. Fuzzy Syst.*, **32** (2024), 2378–2389. https://doi.org/10.1109/TFUZZ.2023.3346927

27. N. Ayyappan, N. Gunasekaran, A. Manivannan, S. Lakshmanan, Finite-time H_∞ boundedness of delayed interconnected systems using sliding mode control with partitioned interval strategy, *Commun. Nonlinear Sci. Numer. Simul.*, **157** (2026), 109673. https://doi.org/10.1016/j.cnsns.2026.109673

28. Y. Chen, X. Zhang, Z. Yan, O. Faydasicok, S. Arik, Sampled-data control for Markovian switching neural networks with output quantization and packet dropouts, *J. Franklin Inst.*, **361** (2024), 107252. https://doi.org/10.1016/j.jfranklin.2024.107252

29. Q. Song, Q. Wu, Y. Liu, Stabilization of chaotic quaternion-valued neutral-type neural networks via sampled-data control with two-sided looped functional approach, *Nonlinear Anal. Modell. Control*, **29** (2024), 1150–1166. https://doi.org/10.15388/namc.2024.29.37852

30. G. Jiang, L. Wang, X. Zong, Q. Xiao, G. Zhang, J. Hu, Practically predefined-time stabilization of stochastic fuzzy memristive neural networks under deception attacks, *IEEE Trans. Cybern.*, **56** (2026), 1071–1082. https://doi.org/10.1109/TCYB.2025.3621274

31. Y. Ni, Z. Wang, Y. Fan, X. Huang, H. Shen, Memory-based event-triggered control for global synchronization of chaotic Lur'e systems and its application, *IEEE Trans. Syst. Man Cybern. Syst.*, **53** (2023), 1920–1931. https://doi.org/10.1109/TSMC.2022.3207353

32. Y. Liu, G. Cui, G. Gao, Event-triggered synchronization control for neural networks against DoS attacks, *Electron. Res. Arch.*, **33** (2025), 121–141. https://doi.org/10.3934/era.2025007

33. Y. Liu, Z. Fang, J. H. Park, F. Fang, Quantized event-triggered synchronization of discrete-time chaotic neural networks with stochastic deception attack, *IEEE Trans. Syst. Man Cybern. Syst.*, **53** (2023), 4511–4521. https://doi.org/10.1109/TSMC.2023.3251355

34. J. Zhou, X. Ma, Z. Yan, S. Arik, Non-fragile output-feedback control for time-delay neural networks with persistent dwell time switching: A system mode and time scheduler dual-dependent design, *Neural Networks*, **169** (2024), 733–743. https://doi.org/10.1016/j.neunet.2023.11.007

35. T. Bu, Quantized H_∞ synchronization for Hopfield networks subject to time-variable delay, *Networks Heterogen. Media*, **20** (2025), 1392–1410. https://doi.org/10.3934/nhm.2025060

36. Z. Yan, X. Huang, J. Liang, Aperiodic sampled-data control for stabilization of memristive neural networks with actuator saturation: A dynamic partitioning method, *IEEE Trans. Cybern.*, **53** (2023), 1725–1737. https://doi.org/10.1109/TCYB.2021.3108805

37. C. Ge, X. Liu, Y. Liu, C. Hua, Event-triggered exponential synchronization of the switched neural networks with frequent asynchronism, *IEEE Trans. Neural Networks Learn. Syst.*, **35** (2024), 1750–1760. https://doi.org/10.1109/TNNLS.2022.3185098

38. Y. Liu, Z. Wang, X. Huang, H. Shen, Multisynchronization of coupled multistable neural networks via event-triggered impulsive control and its application to associative memory, *IEEE Trans. Autom. Sci. Eng.*, **22** (2025), 6729–6739. https://doi.org/10.1109/TASE.2024.3453294

39. K. Gu, V. L. Kharitonov, J. Chen, *Stability of Time-Delay Systems*, 1^{st} edition, Birkhäuser, 2003. https://doi.org/10.1007/978-1-4612-0039-0

40. A. Seuret, F. Gouaisbaut, Wirtinger-based integral inequality: Application to time-delay systems, *Automatica*, **49** (2013), 2860–2866. https://doi.org/10.1016/j.automatica.2013.05.030

AIMS Press